FLUTTER OF ASYMMETRICALLY SWEPT WINGS

by

Terrence A. Weisshaar*

and

J.B. Crittenden+

Virginia Polytechnic Institute

and State University

Blacksburg, Virginia

This research was supported by NASA Ames Research Center, Moffett Field, California under NASA Grant NSG-2016.

Index categories: Aircraft Handling, Stability and Control; Aeroelasticity; Aircraft Structural Design.

*Assistant Professor, Aerospace and Ocean Engineering Department, Member, AIAA.

+Research Assistant, Aerospace and Ocean Engineering Department, Member, AIAA.

FLUTTER OF ASYMMETRICALLY SWEPT WINGS

By

Terrence A. Weisshaar
and
J. B. Crittenden

March 12, 1976

Backup Document for AIAA Synoptic Scheduled for Publication in the AIAA Journal, August 1976

Aerospace and Ocean Engineering
Virginia Polytechnic Institute
and State University
Blacksburg, Virginia 24061

SYNOPTIC BACKUP DOCUMENT

This document is made publicly available through the NASA scientific and technical information system as a service to readers of the corresponding "Synoptic" which is scheduled for publication in the following (checked) technical journal of the American Institute of Aeronautics and Astronautics.

- [X] AIAA Journal, August 1976
- [ ] Journal of Aircraft
- [ ] Journal of Spacecraft & Rockets
- [ ] Journal of Hydronautics

A Synoptic is a brief journal article that presents the key results of an investigation in text, tabular, and graphical form. It is neither a long abstract nor a condensation of a full length paper, but is written by the authors with the specific purpose of presenting essential information in an easily assimilated manner. It is editorially and technically reviewed for publication just as is any manuscript submission. The author must, however, also submit a full backup paper to aid the editors and reviewers in their evaluation of the synoptic. The backup paper, which may be an original manuscript or a research report, is not required to conform to AIAA manuscript rules.

For the benefit of readers of the Synoptic who may wish to refer to this backup document, it is made available in this microfiche (or facsimile) form without editorial or makeup changes.

ABSTRACT

Recent interest in asymmetrically swept, or oblique, wings has raised fundamental questions about the aeroelastic stability characteristics of such wings. This paper presents two formulations of the oblique wing flutter problem; one formulation allows only simple wing bending deformations and rigid body roll as degrees of freedom, while the second formulation includes a more complex bending-torsional deformation together with the roll freedom. Flutter is found to occur in two basic modes. The first mode is associated with wing bending-aircraft roll coupling and occurs at low values of reduced frequency. The second instability mode closely resembles a classical bending-torsion wing flutter event. This latter mode occurs at much higher reduced frequencies than the first. The occurrence of the bending-roll coupling mode is shown to lead to lower flutter speeds while the bending-torsion mode is associated with higher flutter speeds. The ratio of the wing mass moment of inertia in roll to the fuselage roll moment of inertia is found to be a major factor in the determination of which of the two instabilities is critical.

Nomenclature

$[a]$ = flexibility matrix for clamped fuselage wing

b_r = wing reference semi-chord

c = wing chord measured perpendicular to elastic axis (Fig. 1)

$\bar{c}$ = wing chord measured parallel to the free stream direction

c_{L_α} = 2-dimensional sectional lift-curve slope

g = structural damping parameter

i = $\sqrt{-1}$

I_o = wing roll moment of inertia at zero sweep

k = reduced frequency, $\omega c/2V_n$ or $\omega\bar{c}/2V$

R = $(I_o/I_T)\cos^2\Lambda$

s = wing semi-span

V = airspeed

V_f = flutter speed

V_n = airspeed normal to swept axis, $V_n = V\cos\Lambda$

Λ = sweep angle

ρ = air density

ω = frequency of oscillation

Introduction

The recent interest in the use of an asymmetrically swept, high-aspect-ratio wing to achieve high lift-to-drag ratios has generated interest in the aeroelastic stability characteristics of such a configuration. However, the undesirable static aeroelastic divergence characteristics of symmetrically swept forward wings has prompted some caution on the part of structural engineers towards the asymmetrical wing. As a result, considerable discussion of the merits of such a design and the potential weight penalties which might be incurred has occurred. Jones and Nisbet (Ref. 1) have presented data which tend to allay some misgivings about the aeroelastic stability of asymmetrically swept or oblique wings. Prominent among their findings is the discovery that the inclusion of the rigid-body roll degree of freedom of the aircraft appears to have a stabilizing effect on the aeroelastic stability of the wing, when compared to the stability of a similar, but clamped, wing. Their analytical results were obtained through the use of quasi-static aerodynamic theory to represent the perturbation lift forces generated by the harmonic motion of their idealized flexible model.

This study seeks to explore, in somewhat more detail than Ref. (1), the flutter behavior of asymmetrically swept or oblique wings; to accomplish this task the results of two studies are presented. The first study examines the flutter behavior of an idealized finite span, uniform-property wing in incompressible flow swept asymmetrically at various angles to the flow. For this portion of the study, quasi-steady aerodynamic strip theory will be employed in the equations of motion; the Galerkin method will be used to solve these equations.

The second portion of tudy entails the use of a more sophisticated approach to the solution of the oblique wing flutter problem. This approach uses a finite-element, unsteady aerodynamic representation together with a multi-degree-of-freedom structural model to examine more closely and more accurately the flutter behavior of variable planform wings. In all cases, the flow is assumed to be incompressible.

From these studies, it will be shown that, at moderate sweep angles, the flutter speed of the wing may be lowered when compared with the flutter speed of the wing at zero sweep. In addition, the shape of the wing planform and the spanwise distribution of stiffness and weight will have a significant effect on the relation between flutter speed and sweep angle.

Discussion

The first part of this study is concerned with the aeroelastic analysis of a simplified oblique wing model, shown in Fig. 1. The impetus for such a study stems from the desirability of assessing the behavior of the flutter speed of the wing as it is asymmetrically swept. This model represents a wing of uniform structural and aerodynamic properties, asymmetrically swept at an angle Λ to the flow. This high-aspect-ratio wing is idealized as a beam with a straight elastic axis, free to roll about an axis parallel to the flow. It is assumed that mass is distributed along this roll axis such that a mass moment of inertia, I_f, simulating the roll moment of inertia of the fuselage, appears concentrated there.

To examine the aeroelastic stability of this model, assume that it is caused to undergo small oscillations about a "wings-level" static equilibrium position. The stability of the subsequent motion can be determined by an examination of the character of this free vibration.

The structural behavior of this wing can be modelled through the use of conventional Euler-Bernoulli beam theory. It is further assumed that the wing has no torsional flexibility so that only bending flexibility is important. The limits to the validity of this latter assumption will be discussed later in this paper.

In Ref. 2 , Barmby, et al. discuss the flutter analysis of symmetrically swept wings through the use of aerodynamic strip theory and the Theodorsen functions. The present study neglects all the noncirculatory aerodynamic terms in Ref. 2, but retains two of the circulatory terms. In addition, the free vibratory motion is assumed to take place at a value of reduced frequency $k = \omega c/2V_n$ which is so small that the flow is quasi-steady. The circulatory aerodynamic terms retained are: a term which corresponds to the familiar damping-in-roll; and a term which arises from the angle of attack generated by bending deformations of a swept wing.

The assumptions about the behavior of this idealized model undergoing small oscillations in the airstream lead to the following differential equation of motion for the elastic wing.

$$m\frac{\partial^2 W}{\partial t^2} + EI\frac{\partial^4 W}{\partial y^4} + (qcc_{L\alpha}\cos^2\Lambda)\frac{\partial W}{\partial y}\tan\Lambda \qquad (1)$$

$$+\left(\frac{qcc_{L\alpha}\cos^2\Lambda}{V\cos\Lambda}\right)\frac{\partial W}{\partial t} - qcc_{L\alpha}\cos^2\Lambda\left(\frac{py}{V}\right)$$

$$- m\dot{p}y\cos\Lambda = 0$$

where m = wing mass per unit length along the y-axis

EI = bending stiffness of cross-section perpendicular to y-axis

q = freestream dynamic pressure

W = wing deformation due to elastic deformation, positive upward

t = time

p = roll rate in radians per unit time

Nondimensionalization of Eq. (1) yields the following equation.

$$\left(\frac{mL^4}{EI}\right)\ddot{w} + \frac{\partial^4 w}{\partial \eta^4} + \lambda \frac{\partial w}{\partial \eta} - \left(\frac{\lambda}{\tan\Lambda}\right)\left(\frac{pL}{V}\right)\eta \tag{2}$$

$$+\left(\frac{\lambda}{\sin}\right)\left(\frac{\dot{w}L}{V}\right) - \left(\frac{mL^4}{EI}\right)(\dot{p}\cos\Lambda)\,\eta = 0$$

where ($\dot{}$) = differentiation with respect to time

$w = W/L$

$\eta = y/L$

$\lambda = qcc_{L_\alpha}L^3\sin\Lambda\cos\Lambda/EI$

The requirement that the sum of all roll moments generated by wing oscillatory motion be equal to zero results in the additional equation:

$$\left(I_f + I_o\cos^2\Lambda\right)\dot{p} = \left(qcc_{L_\alpha}L^2\cos^3\Lambda\right)\left(\int_{-1}^{1}\frac{\partial w}{\partial \eta}\,\eta d\eta\right)\tan\Lambda \tag{3}$$

$$+\left(mL^3\cos\Lambda\right)\int_{-1}^{1}\ddot{w}\eta d\eta$$

$$-\frac{2}{3}qcc_{L_\alpha}L^2\cos^3\Lambda\left(\frac{pL}{V}\right)$$

$$+\frac{qcc_{L_\alpha}L^3\cos^2\Lambda}{V}\int_{-1}^{1}\dot{w}\eta d\eta$$

If we let $\phi = p\cos\Lambda$ then Eq. (3) may be written as

$$\ddot{\phi} + \frac{2}{3}\left(\frac{\gamma L}{V}\right)\dot{\phi} = (\gamma\sin\Lambda)\int_{-1}^{1}\frac{\partial w}{\partial \eta}\,\eta d\eta + \frac{3}{2}\left(\frac{I_W}{I_T}\right)\int_{-1}^{1}\ddot{w}\eta d\eta \tag{4}$$

$$+\left(\frac{\gamma L}{V}\right)\int_{-1}^{1}\dot{w}\eta d\eta$$

where $I_T = I_f + I_o\cos^2\Lambda$

$I_W = I_o\cos^2\Lambda = \frac{2}{3}mL^3\cos^2\Lambda$

$\gamma = qcc_{L_\alpha}L^2\cos^3\Lambda/I_T$

To solve Eqs. (2) and (4), the time dependency is eliminated by recognition that the functions $w(\eta,t)$ and $\phi(t)$ are separable such that

$$w(\eta,t) = f(\eta)e^{rt} \tag{5a}$$

$$\phi(t) = \phi e^{rt}$$

Next, Eq. (2) is separated into two parts, one valid in the region $-1 \leq \eta \leq 0$, the other valid in the region $0 \leq \eta \leq 1$. Finally the resulting set of equations is solved approximately through use of Galerkin's method. A simple polynomial to use for such a solution is that shape obtained for uniform loading of a cantilever beam. In this case the function $f(\eta)$ is approximated as:

$$f(\eta) = \begin{cases} \frac{a}{3}(6\eta^2 - 4\eta^3 + \eta^4) & 0 \leq \eta \leq 1 \\ \frac{b}{3}(6\eta^2 + 4\eta^3 + \eta^4) & -1 \leq \eta \leq 0 \end{cases} \tag{6}$$

where a and b are unknown constants. The Galerkin method leads to a set of three homogeneous algebraic equations, represented in matrix form as:

$$\left[d_{ij}\right] \begin{Bmatrix} a \\ b \\ \Phi \end{Bmatrix} = \begin{Bmatrix} 0 \\ 0 \\ 0 \end{Bmatrix} \tag{7}$$

The coefficients d_{ij} are given in the Appendix to this paper.

It is found that, in the absence of the roll freedom, the first natural frequency of vibration of the clamped wing, <u>in vacuo</u>, is predicted by the Galerkin method to be

$$\omega_o = 3.530 \sqrt{\frac{EI}{mL^4}} \tag{8}$$

This compares with the exact solution (Ref. 3)

$$\omega_o = 3.518 \sqrt{\frac{EI}{mL^4}} \tag{9}$$

For the clamped wing, it is found that the sweptforward wing undergoes static divergence when r is zero. This occurs at a value of λ equal to

6.40. The exact solution gives a value of λ for static divergence of 6.33 (Ref. 4).

If all the system parameters, such as EI, Λ and V, are substituted into the expressions for d_{ij}, then the determinant of the matrix $[d_{ij}]$, written as $\Delta(d_{ij})$, can be used to find r through the relation:

$$\Delta(d_{ij}) = 0 \tag{10}$$

With reference to Eqs. (5a,b), it is seen that if r is found to be a real number, then motion is aperiodic. A positive real value of r indicates aperiodic instability or static divergence. On the other hand, if r is found to be a complex number, motion is harmonic. If $r = \alpha + i\omega$ then the motion is periodic with frequency ω. For negative values of α, the motion decays, but for positive values of α it grows with time. This latter situation corresponds to the dynamic aeroelastic instability commonly referred to as wing flutter. At the value $r = i\omega$, the system undergoes undamped oscillation and is said to be in neutral equilibrium. For a given set of system parameters, the airspeed V at which this occurs is termed the flutter speed, V_F.

The way in which the problem is presently formulated allows the selection of one system parameter as the unknown in Eq. (10). The magnitude of the complex number r is of no interest, but rather the value of velocity at which neutral stability occurs. For this reason, it is found to be advantageous to let $r = i\omega$ in the expressions for d_{ij} and to express these coefficients in terms of ω_o and the parameter β, defined as

$$\beta = \lambda/\lambda_{div} \tag{11a}$$

where

$$\lambda_{div} = 32/5 = 6.40 \tag{11b}$$

Given the system physical parameters, the determinant in Eq. (10) may be expressed in terms of the independent variable β. Collecting terms, the determinant is found to have a real part and an imaginary part given respectively by the expressions

$$\left(\frac{\omega}{\omega_o}\right)^4\left[1-\frac{39}{40}R\right]-\left(\frac{\omega}{\omega_o}\right)^2\left[2\left(1-\frac{39}{80}R\right)+\frac{\psi D}{30}+D^2\omega_o^2\left(1-\frac{39}{40}R\right)\right] \quad (12a)$$

$$+\left[1-\beta^2+\frac{26}{25}\beta R+\frac{41}{60}\psi D\right]=0$$

and

$$\left(\frac{\omega}{\omega_o}\right)^4\left(1-\frac{77}{80}R\right)-\left(\frac{\omega}{\omega_o}\right)^2\left(1+\frac{1}{40}R+\frac{1}{120}\psi D\right) \quad (12b)$$

$$+\frac{R}{2}\left(1+\beta^2/25\right)=0$$

where

$$D^2\omega_o^2=\frac{104}{405}\left(\frac{\rho c c_{L\alpha} L}{2m}\right)\left(\frac{\beta R}{\tan\Lambda}\right) \quad (13a)$$

and

$$\psi D=\frac{104}{305}\left(\frac{\rho c c_{L\alpha} L}{2m}\right)\left(\frac{R}{\tan\Lambda}\right) \quad (13b)$$

The selection of a value of β which yields identical values of the ratio ω/ω_o in Eqs. (12a,b) completes the solution. With this value of β, the flutter velocity then may be obtained.

The above solution procedure was implemented for a small model wing constructed of aluminum sheet with a constant thickness of 0.064 inches. The wing properties were taken to be:

Material density = 0.101 lb_m/in^3

c = 4 in. L = 20 in. $c_{L\alpha} = 2\pi$

$I_o/I_f = 3$ EI = 874.0 lb_f-in.

Using a sea level air density value, Eqs. (12a, b) were solved numerically using a Newton's Method trial and error solution technique. The results of this analysis are shown in Fig. 2.

From Fig. 2, it is seen that the flutter speed decreases as the wing is swept. For small values of Λ, the value of V_F greatly exceeds that of the clamped-wing static divergence speed, V_D. However, as Λ increases, the critical speeds V_F and V_D draw closer together; at $\Lambda = 90°$ they will coincide. As suggested by Jones and Nisbet in Ref. 1, the moment of inertia ratio I_W/I_T plays a significant role in the flutter analysis of this asymmetric wing. From the expression for I_W/I_T given below Eq. (4), it is seen that this ratio tends to zero as Λ approaches 90°. It has been suggested that this mass moment of inertia ratio should be as large as possible to improve flutter performance. The results in Fig. 2 support this observation.

Since one of the original assumptions of the present analysis was that the flutter instability occurs at relatively small values of reduced frequency k, it is worthwhile to note the values of reduced frequency for which the instabilities in Fig. 2 occur. These numbers are listed in Table I. Although these reduced frequencies are reasonably small, the accuracy of these results is probably degraded somewhat by the quasi-steady flow assumption.

The model just analysed is similar to, but not identical to, a series of models used by Papadales (Ref. 5) in wind tunnel experiments at Virginia Polytechnic Institute. Those experiments had as their primary objective the study of the static aeroelastic characteristics of clamped oblique wings. However, when those tests were completed, simple flutter tests were conducted on roll-free models. Although no attempt to take accurate data was made during these flutter demonstration tests, the velocity magnitudes shown in Fig. 2 correspond to the order of magnitude of the velocities observed in these demonstrations. In addition, for

sweep angles greater than 15-20^0, the primary mode of instability was observed to be primarily a fundamental symmetrical bending mode coupled with the asymmetrical rigid body roll oscillation.

For sweep angles less than about 20^0, the tests described in Ref. 5 found a flutter mode which resembled a more conventional "fixed-root" bending-torsion instability. These observations, together with the desire to obtain a more accurate versatile analysis model, suggested the application of a more sophisticated analysis technique to the oblique wing flutter problem. It is to this analysis that attention is now turned.

Conventional flutter analysis of realistic aircraft employs assumed structural deflections or mode shapes together with generalized coordinates assigned to these mode shapes. An excellent discussion of modal and non-modal matrix methods of flutter analysis is given by Rodden in Ref. 6. In addition, Ref. 6 presents a succinct discussion of how to include free-free boundary conditions into the conventional restrained or clamped model. This latter discussion follows the development given in Ref. 7, but is more general. The highlights of Ref. 6 are reviewed here.

To analyze the flutter behavior of a planform such as that shown in Fig. 4, it is necessary that the following items be taken into account: the distributed mass of the wing along the span; the variable bending and torsional stiffness along the span; and the unsteady, three-dimensional aerodynamic forces and moments associated with deformations caused by wing oscillations. With the assumption of simple harmonic motion at frequency ω, the classical matrix equation for flutter analysis, before the inclusion of assumed modes, is given by (Ref. 6):

$$\left\{h\right\} = \left(\frac{\omega^2}{1 + ig}\right)\left[a\right]\left[\left[M\right] + \rho b_r^2 s\left[C_h\right]\right]\left\{h\right\} \qquad (14)$$

In this equation the static flexibility matrix [a] has been divided by the factor (1 + ig) to account for the structural damping necessary to sustain simple harmonic motion. The elements of the vector {h} are actual elastic deflections and rotations at control points on the wing. The mass matrix [M] and aerodynamic influence coefficient matrix $[C_h]$ are both multiplied by the frequency squared. The elements of $[C_h]$ are complex numbers and functions of Mach number and the local control point reduced frequency, $k = \omega b/V$, where b is the local semi-chord. With the formulation in Eq. 14, the unsteady aerodynamic forces enter into the problem, mathematically, as complex masses.

The idealization of the wing structure as an assemblage of beams, each with a straight elastic axis, permits the use of conventional finite element structural analysis methods to describe the wing stiffness and flexibility. The reader is referred to Refs. 8 and 9 for discussions of this metho' Similarly, the mass matrix may be formulated from finite element methods. The mass matrix must account for the fact that the wing shear centers may be offset from the wing chordwise location of the centers of mass. Finally, to model the three-dimensional aerodynamic forces and moments, a doublet-lattice method (Ref. 10) was used to generate aerodynamic influence coefficients. To expedite these calculations, an existing computer program (Ref. 11) was used.

A computer program was written to calculate the matrices in Eq. 14. The free vibration modes for the clamped system are then used to condense the matrix equations. The free-free boundary conditions are then introduced to "free" the clamped system described in Eq. 14; this allows rigid body roll freedom. Once these matrices have been formed, the eigenvalues and eigenvectors may be found. Since the aerodynamic

influence coefficients are functions of reduced frequency k and Mach number (in these studies, Mach number is zero), a set of eigenvalues and eigenvectors corresponding to each value of k is generated. The familiar V-g method (Ref. 3, pp. 565-568) is then used to find the value of velocity at which neutral stability occurs.

To assess the effect of torsion and unsteady aerodynamics on the flutter analysis of the oblique wing, the uniform property aluminum wing was again analyzed. The wing is considered to have the same structural properties as before, but, in the present example, GJ is taken to be equal to 1346 lb-in. It should be noted that the flat, sheet-aluminum wing has a ratio of first bending to first torsion which is slightly higher than that common to conventional aircraft.

The analysis of the constant property wing, including roll freedom and torsional flexibility and employing the doublet-lattice method was conducted with a sixty degree-of-freedom model. These sixty degrees of freedom were obtained by considering ten control points on each wing; each control point has pitch, plunge and bending rotation elastic degrees of freedom. This model was subsequently reduced to a twenty degree-of-freedom model by using the first twenty natural modes of the system.

The results of this flutter analysis are displayed in Fig. 3 as ratios of the instability velocity (either flutter or divergence) to the velocity at which wing torsional divergence occurs at zero sweep; this latter velocity is denoted as V_{DO}.

In Fig. 3 the behavior of the wing when the fuselage is clamped is shown as the curve labelled V_D/V_{DO}. With the fuselage clamped, instability is found to occur at a reduced frequency $k \cong 0$; this is divergence. When roll freedom is allowed, and when $I_o/I_f = 3$, a dynamic instability appears; this is flutter and is shown as the curve V_F/V_{DO}. Unlike the

previous results, the flutter speed does not tend to infinity as Λ tends to zero. This analysis reveals that the wing has two possible modes of flutter instability. The first type of instability is characterized by a classical bending-torsion oscillation of the wing with its root fixed or clamped. The second mode of instability is one which involves bending-torsion deformation coupled with a significant amount of rigid body roll. Depending upon the sweep angle, one of these modes will occur before the other as airspeed is increased.

For the example shown in Fig. 3, the bending-torsion-roll mode does not become critical until the sweep angle is near 15^0. The cusp in the V_F vs. Λ curve indicates that the mode of instability changes at this point. Also, the flutter frequency will change discontinuously at this point.

Gaukroger (Ref. 12) has noted a similar phenomenon associated with the pitching degree of freedom on bilaterally symmetric aircraft. A phenomenon termed "body-freedom flutter" is found to occur if the aircraft pitching moment of inertia is small enough. For large values of pitch inertia, a type of wing flutter resembling a "wing-clamped" instability occurs. This latter type of flutter is termed "fixed-root flutter." The flutter frequency at which body-freedom flutter occurs is significantly lower than that at which fixed-root flutter occurs. It is also shown that for bilaterally symmetric aircraft antisymmetrical body-freedom flutter involving rigid-body roll is theoretically possible, but only for cases where the fuselage roll moment of inertia is extremely small or negative in comparison to that of the wing. These results are contrasted with the present results in which body-freedom flutter occurs if the fuselage moment of inertia is large when compared to that of the wing.

As a further illustration of the flutter behavior of oblique wings, a non-uniform wing planform, constructed of the same material as the uniform property wing, was analyzed. This wing (Fig. 4) has a modified elliptical planform. In this case, the wing-fuselage combination has a roll moment of inertia ratio $I_o/I_f = 11.69$. Fig. 5 shows the stability behavior of the clamped and roll-free wings. While the decrease in divergence speed with increasing Λ for the clamped wing shown in Fig. 4 resembles that of the uniform property wing, the behavior of the flutter speed for the nonuniform wing is much different. Once again, for large sweep angles, the decrease of flutter speed with sweep angle is seen in Fig. 5; however, the roll-free flutter speeds and clamped divergence speeds are more widely separated in Fig. 5 than in Fig. 3.

To assess the obvious importance of the fuselage roll moment of inertia, the aeroelastic stability of the nonuniform property wing shown in Fig. 4 is again studied. However, the roll moment of inertia of the fuselage is now increased by a factor of two. The results of this study are presented in Fig. 6 and are compared to those previously obtained using the smaller fuselage roll moment of inertia. Once again, the results are displayed as ratios of flutter speed to clamped divergence speed at zero sweep angle.

The effect of increasing the fuselage roll moment of inertia is clearly seen in Fig. 6. The flutter speeds for both moment of inertia ratios are seen to be nearly identical until about 15 degrees of sweep. Near this point, the flutter mode for the $I_o/I_f = 5.85$ wing changes from the fixed-root type to the body-freedom type. This is seen to depress the flutter speed as Λ increases.

As a final example, consider the uniform property aluminum wing. This wing has been previously analyzed using a quasi-steady strip theory model with elastic bending degrees of freedom and roll coupling. It has also been analyzed with a bending-torsion model which used the doublet-lattice aerodynamic loads. For the present example, the value of the torsional stiffness GJ is chosen to be 10 times that of the example whose results were presented in Fig. 3. The results of the present study are shown in Fig. 7, where they are compared with those presented in Fig. 3. In Fig. 7, the designation "Wing 2" refers to a uniform property wing with properties identical to those of "Wing 1" except that the wing sectional torsional stiffness of Wing 2 is ten times that of Wing 1.

In Fig. 7, the relation between flutter speed and Λ for Wing 2 has an apparent discontinuity near $\Lambda = 15^{0}$. Increasing the value of GJ is found to have a pronounced effect on flutter speed at moderate sweep angles, but has little effect on flutter at high sweep angles. There is a drastic change in the flutter speed near 15 degrees sweep. For sweep angles beyond 15^{0}, the results obtained for this wing with high torsional stiffness resemble those obtained with the bending model and strip theory airloads. The reduced frequencies at the onset of flutter of Wing 2 are displayed in Table II for several sweep angles. From this table, it is seen that the flutter which occurs primarily as a body-freedom instability occurs at relatively low reduced frequencies when compared with the reduced frequencies which arise at the onset of bending-torsion flutter. Also, a comparison of the reduced frequencies in Tables I and II shows that the reduced frequencies at flutter in the two studies are comparable in magnitude.

Conclusions

Before summarizing the results of this paper and listing conclusions, certain features of the idealized models studied should be reviewed. These models were chosen for analysis because of past experience with wind tunnel tests. A constant thickness, sheet-metal wing has a bending stiffness which is proportional to the wing chord measured perpendicular to the wing elastic axis; the torsional stiffness varies in a similar manner. This proportionality of the stiffness to the wing chord leads to bending and torsional stiffness distributions which are concave downward when plotted versus the spanwise coordinate. In actuality, the bending stiffness distribution which results from considerations of wing strength usually appears to have a concave upward distribution (cf. Ref. 3, p. 45).

The wings considered in this study had wing sectional centers of mass coincident with the shear centers; thus, there was no elastic axis-c.g. offset. Dynamic coupling was either nonexistent, as in the case of the uniform property wing, or minimal, as in the case of the variable property wing. This latter wing has a line of shear centers which is curved slightly forward when the wing is in its unswept position.

The combinations and permutations of the various parameters which affect the aeroelastic stability of an aircraft are seemingly endless. However, several conclusions may be drawn from the present studies at zero Mach number. Prominent among these conclusions is that the inclusion of the rigid-body roll degree of freedom into the flutter model causes the critical mode of instability to change from an aperiodic instability (divergence) to an oscillatory instability (flutter). The degree to which the stability boundary is modified depends to a large

extent upon the sweep angle Λ and the ratio of the moments of inertia in roll of the aircraft fuselage and the wing in its unswept position.

If the wing instability appears as a coupling between wing bending-torsion deformation and rigid-body roll (the body-freedom mode), flutter speed is reduced as Λ increases. However, if the system parameters are such that flutter appears primarily as a fixed-root bending-torsion instability, the flutter speed may actually increase as the wing is swept. If the wing can be either elastically or dynamically tailored, it may be possible to avoid the "body-freedom" mode type of instability altogether.

Topics warranting further investigation include: the effect of Mach number on oblique wing flutter; the significance of elastic axis - c.g. offset; and the effect of elastic tailoring of the wing. It is anticipated that these and other studies will provide further insight into this unique aerodynamic design.

REFERENCES

1. Jones, R.T. and Nisbet, J.W., "Transonic Transport Wings — Oblique or Swept?," Astronautics and Aeronautics, Vol. 12, No. 1, January 1974, pp. 40-47.
2. Barmby, J.G., Cunningham, H.J. and Garrick, I.E., "Study of Effects of Sweep on the Flutter of Cantilever Wings," NACA Report 1014, 1951.
3. Bisplinghoff, R.L., Ashley, H. and Halfman, R.L., Aeroelasticity, Addison-Wesley, Reading, Mass., 1955, p. 77.
4. Bisplinghoff, R.L. and Ashley, H., Principles of Aeroelasticity, John Wiley and Sons, New York, 1962, p. 313.
5. Papadales, B.S., An Experimental Investigation of Oblique Wing Static Aeroelastic Phenomena, Master of Science Thesis, Virginia Polytechnic Institute and State University, Blacksburg, Virginia, 1975.
6. Rodden, W.P., "A Matrix Approach to Flutter Analysis," Sherman Fairchild Fund Paper No. FF-23, Institute of the Aeronautical Sciences, 1959.
7. Scanlan, R.H. and Rosenbaum, R., Aircraft Vibration and Flutter, Dover Publications, New York, 1968.
8. Przemieniecki, J.S., Theory of Matrix Structural Analysis, McGraw-Hill, New York, 1968.
9. Gallagher, R.H., Finite Element Analysis Fundamentals, Prentice-Hall, Englewood Cliffs, New Jersey, 1975.
10. Albano, E. and Rodden, W.P., "A Doublet-Lattice Method for Calculating Lift Distributions on Oscillating Surfaces in Subsonic Flows," AIAA Journal, Vol. 7, No. 2, February 1969, pp. 279-285.

11. Giesing, J.P., Kalman, T.P., Rodden, W.P., "Subsonic Unsteady Aerodynamics for General Configurations, Part I, Vol. II, Direct Application of the Nonplanar Doublet-Lattice Method," AFFDL-TR-71-5, November 1971, Wright-Patterson AFB, Ohio.

12. Gaukroger, D. R., "Wing Flutter," AGARD Manual on Aeroelasticity, Part V, Chapter 2, February, 1960.

Table I - Reduced Frequency k at Flutter (Fig. 2)

$k = \omega c/2V_n$	Λ (Degrees)
0.0225	15
0.0330	30
0.0494	45
0.0587	60

Table II - Reduced Frequency k at Flutter

(Wing 2, Fig. 7)

$k = \omega \bar{c}/2V$	Λ (Degrees)
0.29	0.
0.29	7.5
0.29	15
0.022	20
0.025	25
0.028	30
0.038	45
0.045	60

Appendix

The application of Galerkin's method to Eqs. (2,3) results in the determinant of Eq. 10. The elements of the matrix $\left[d_{ij}\right]$ are given below.

$$d_{11} = -\left(\frac{\omega}{\omega_o}\right)^2 + i\omega D + 1 + \beta \tag{A1}$$

$$d_{12} = 0 \tag{A2}$$

$$d_{13} = \frac{9}{8}\left[\left(\frac{\omega}{\omega_o}\right)^2 - i\omega D\right] \tag{A3}$$

$$d_{21} = 0 \tag{A4}$$

$$d_{22} = -\left(\frac{\omega}{\omega_o}\right)^2 + i\omega D + 1 - \beta \tag{A5}$$

$$d_{23} = -\frac{9}{8}\left[\left(\frac{\omega}{\omega_o}\right)^2 - i\omega D\right] \tag{A6}$$

$$d_{31} = \omega^2(13R/30) - i\omega\psi(13/45) - (\gamma\sin\Lambda)(3/5) \tag{A7}$$

$$d_{32} = -\omega^2(13R/30) + i\omega\psi(13/45) - (\gamma\sin\Lambda)(3/5) \tag{A8}$$

$$d_{33} = -\omega^2 + i\omega\psi(2/3) \tag{A9}$$

The following definitions of terms are used in the above equations.

$D = (13/162)(\lambda L/V\sin\Lambda)$ $\qquad$ $\psi = \gamma L/V$

$R = (I_o/I_T)\cos^2\Lambda$ $\qquad$ $\lambda = qcc_{L\alpha}L^3\sin\Lambda\cos\Lambda/EI$

$\beta = \lambda/\lambda_{cr} = 5\lambda/16$ $\qquad$ $\gamma = qcc_{L\alpha}L^2\cos^3\Lambda/I_T$

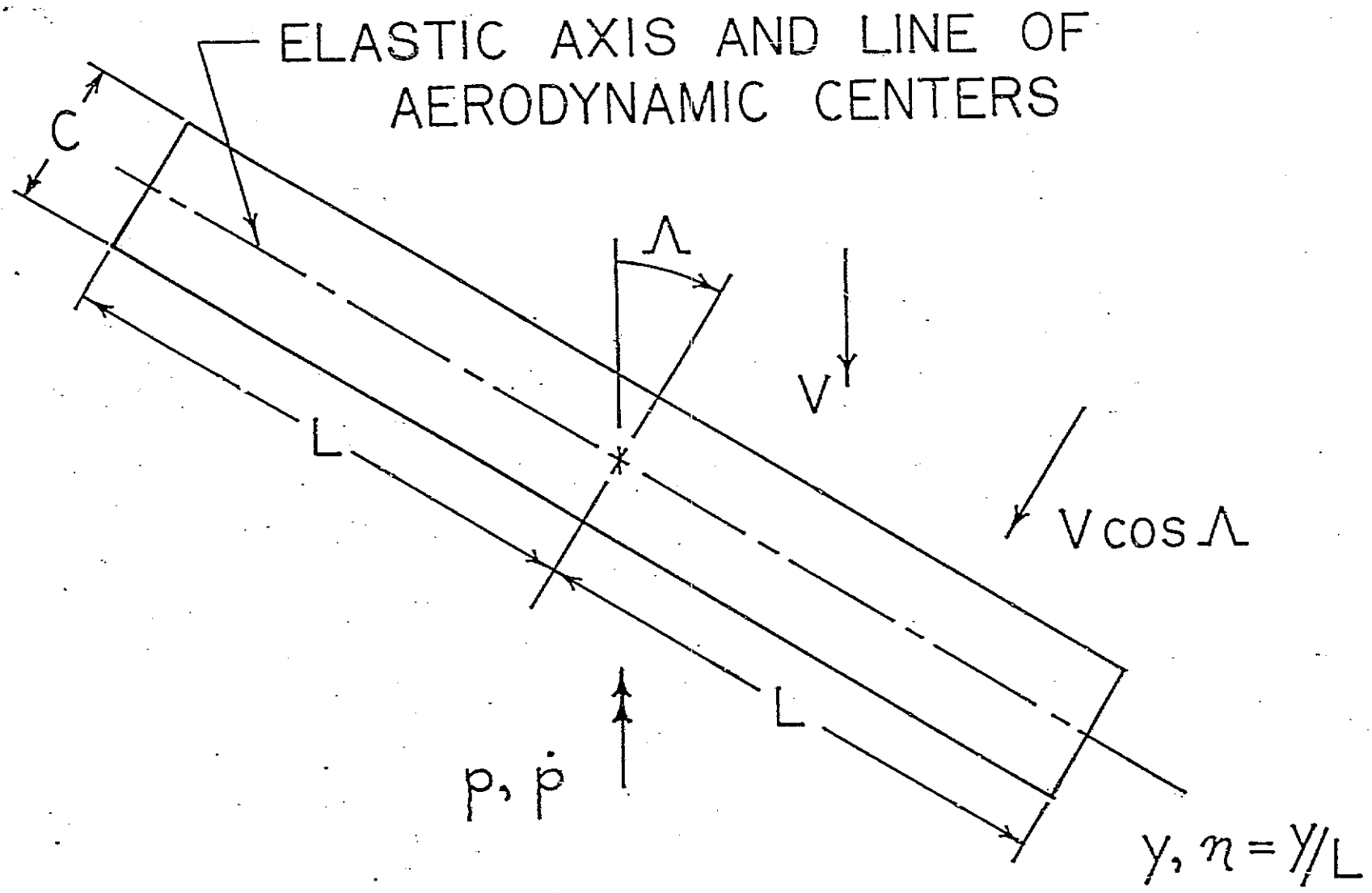

Fig. 1 - Uniform Property Wing; Definition of Geometrical Parameters.

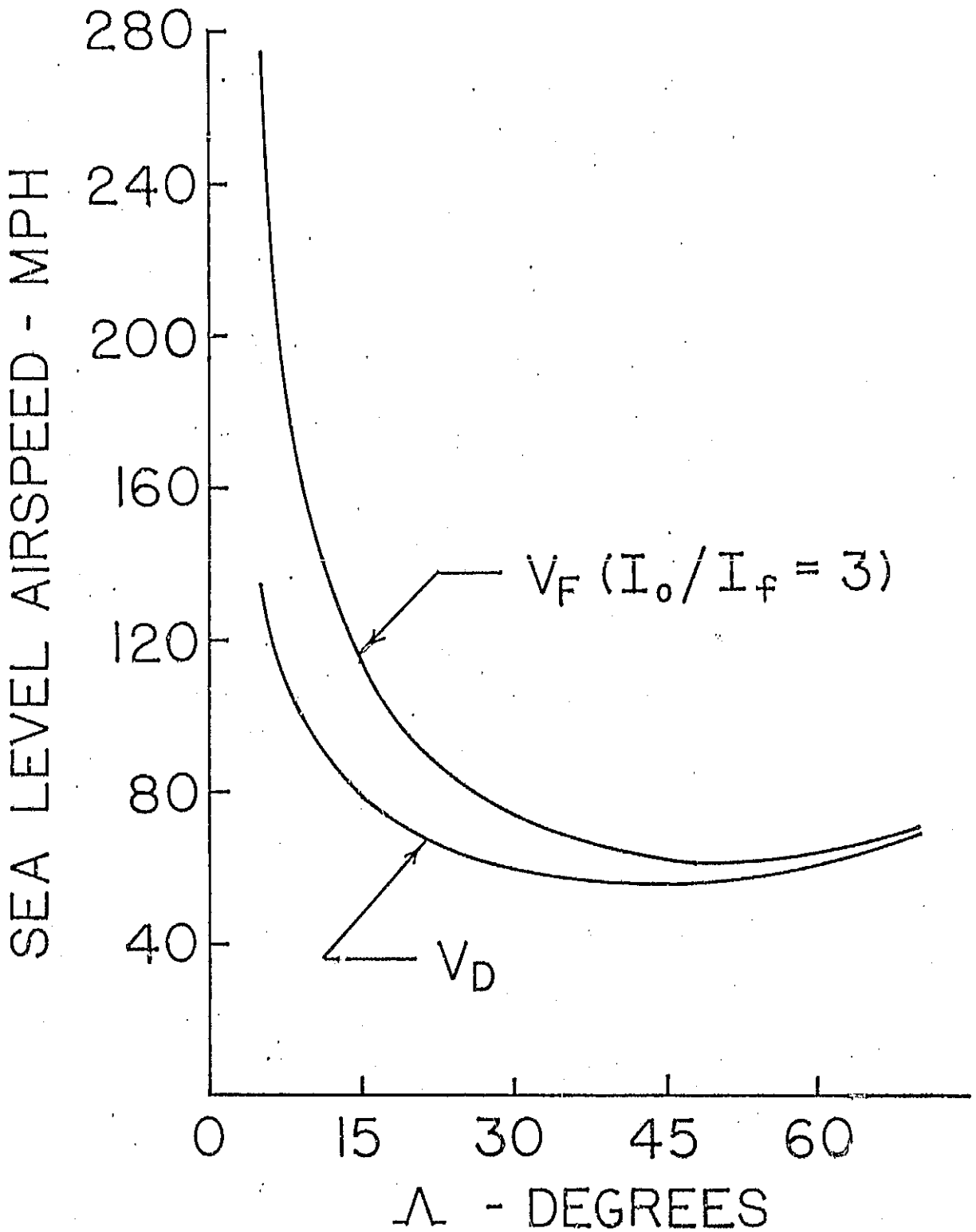

Fig. 2 - Strip Theory Prediction of Flutter Speed V_F Versus Sweep Angle Λ and Divergence Speed V_D Versus Λ.

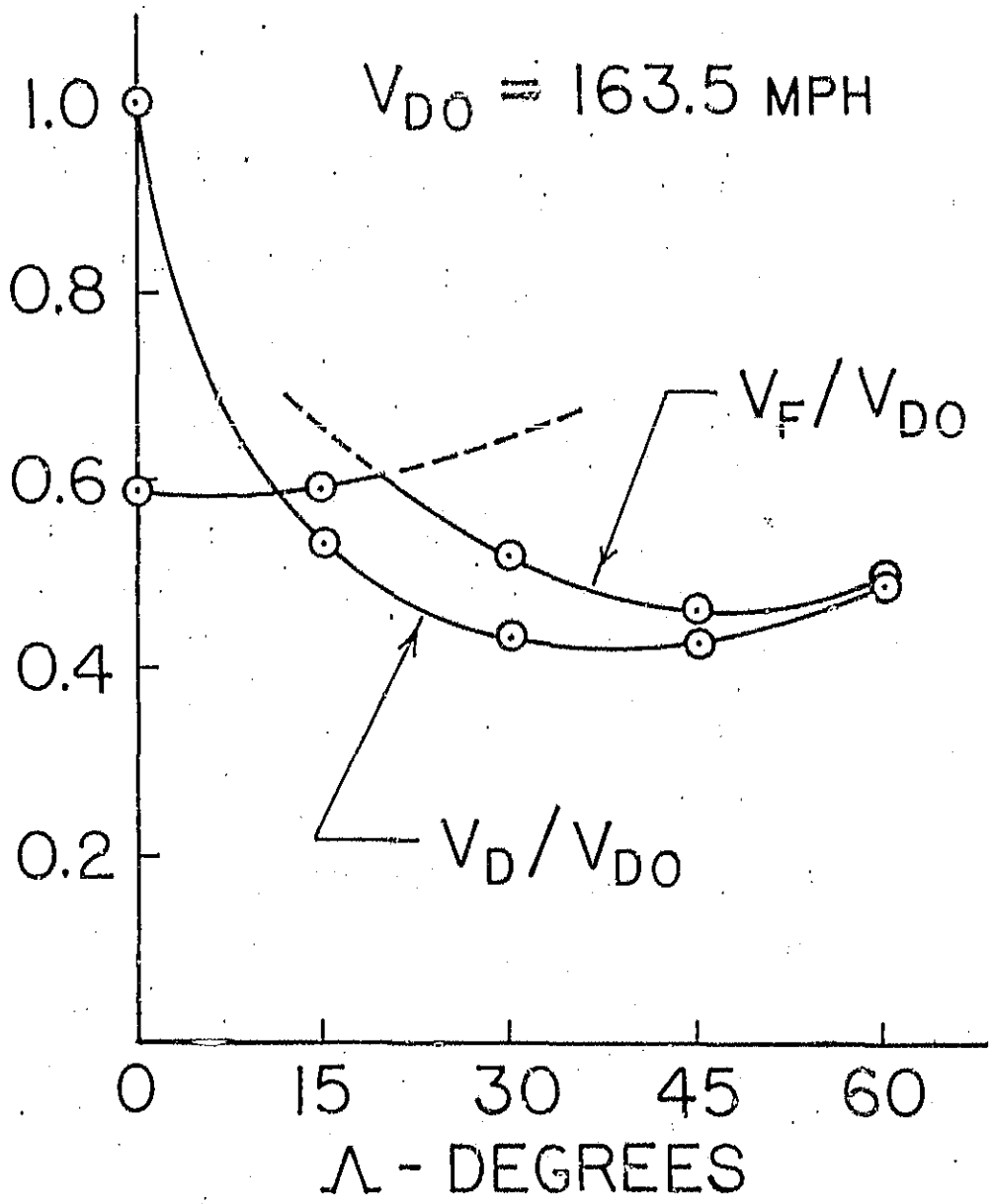

Fig. 3 - Ratio of Aeroelastic Instability Velocity to Divergence Velocity at Zero Sweep Angle, V_{DO}; Uniform Property Wing With Bending-Torsion Flexibility; Doublet-Lattice Aerodynamics.

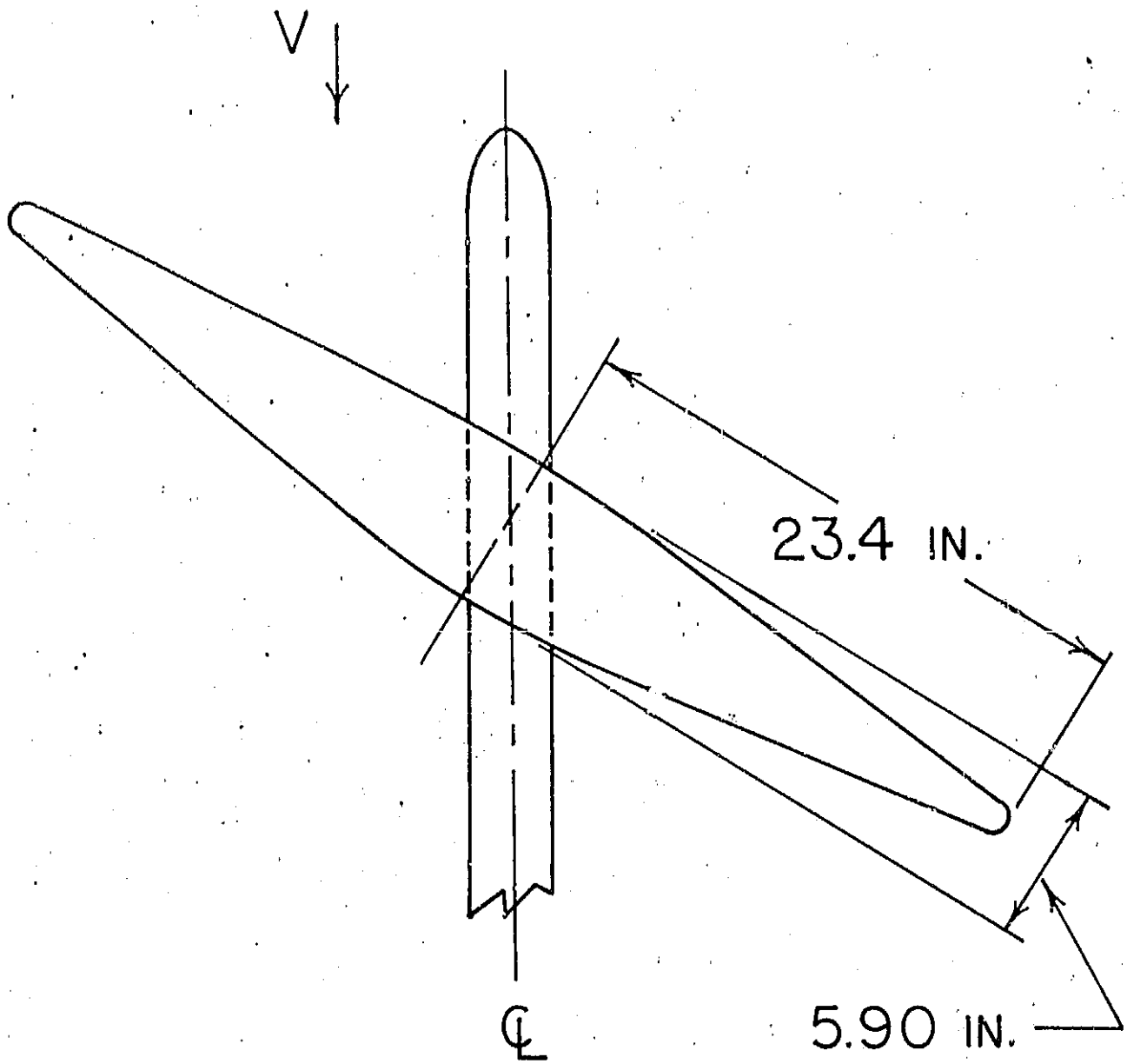

Fig. 4 - Nonuniform Wing Planform.

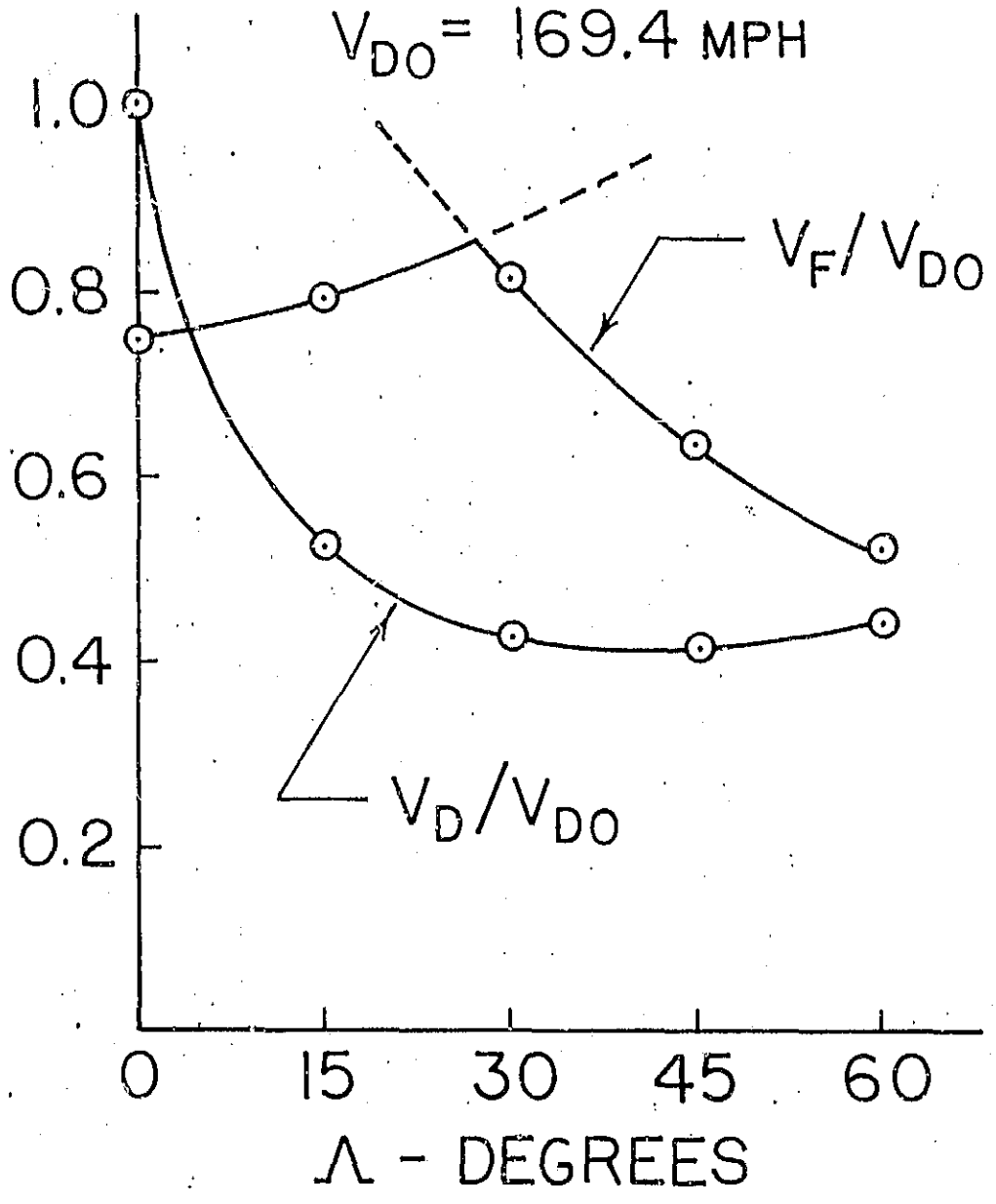

Fig. 5 - Ratio of Aeroelastic Instability Velocity to Clamped Divergence Velocity at Zero Sweep Angle; Nonuniform Wing Planform With Bending-Torsion Flexibility.

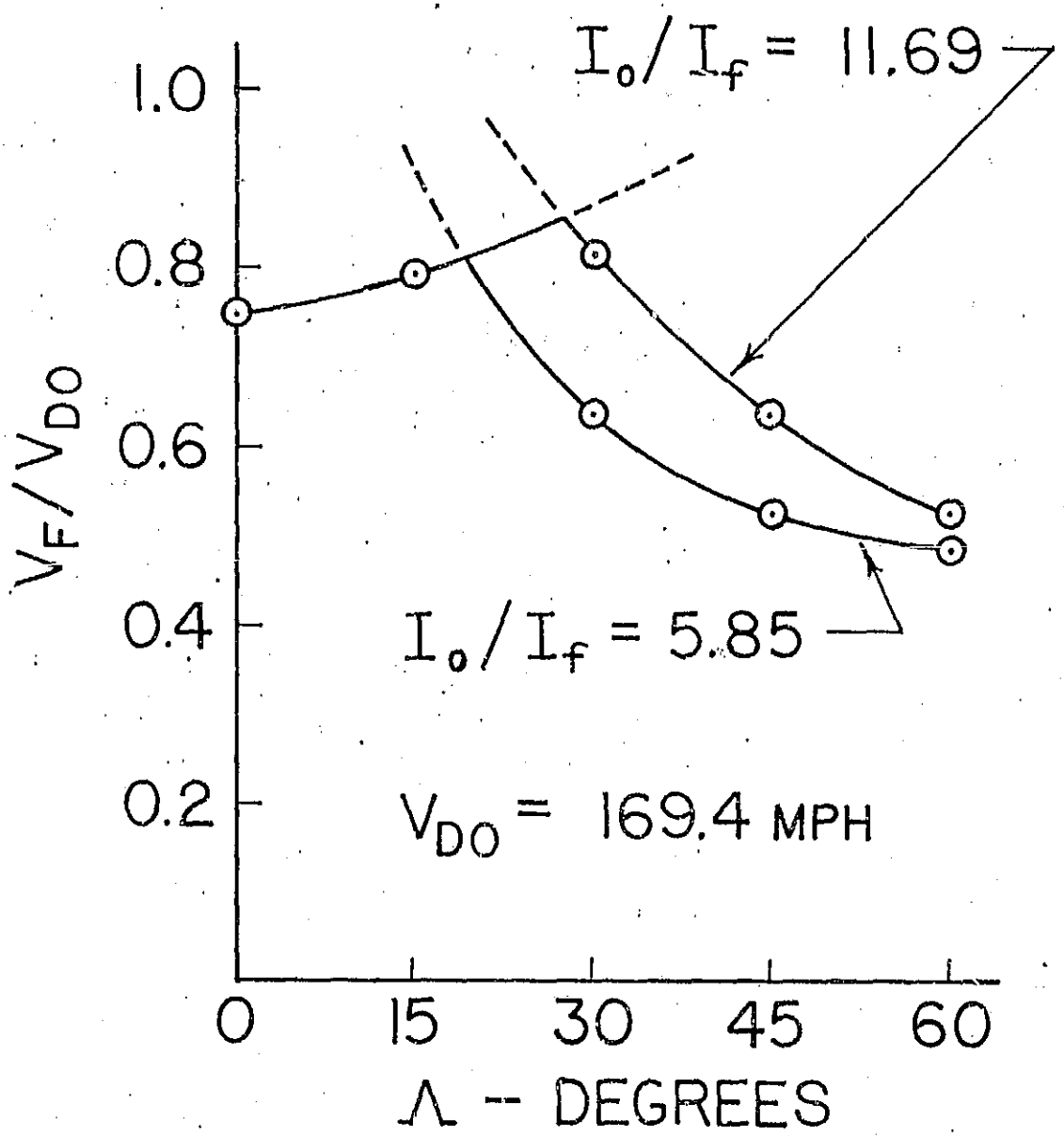

Fig. 6 - The Effect on Flutter of Doubling the Fuselage Moment of Inertia.

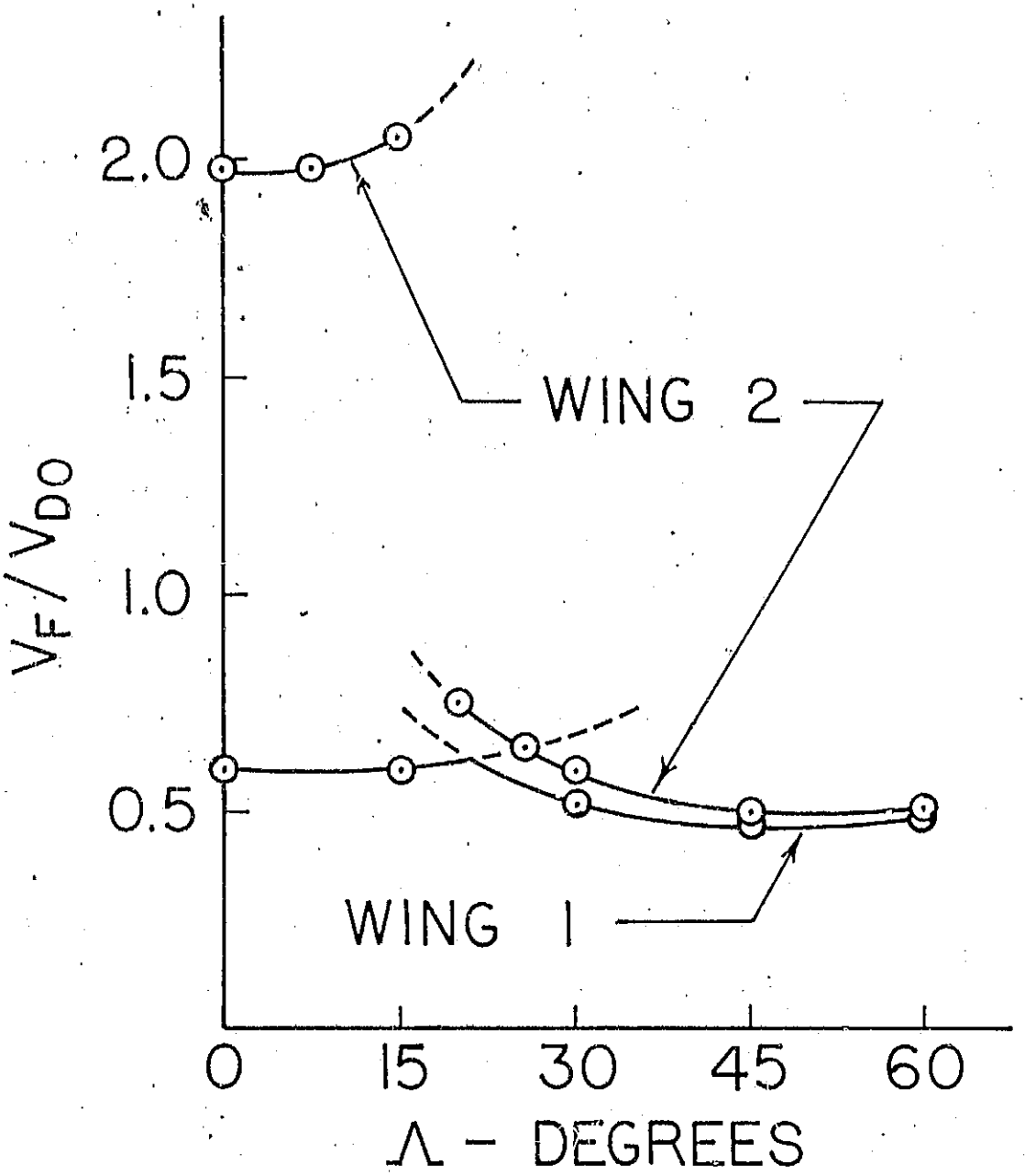

Fig. 7 - The Effect of Greatly Increasing the Torsional Stiffness Distribution of a Uniform Property Wing; Torsional Stiffness Distribution of Wing 2 is 10 Times That of Wing 1.